Effective Chromium Adsorption From Aqueous Solutions and Tannery Wastewater Using Bimetallic Fe/Cu Nanoparticles: Response Surface Methodology and Artificial Neural Network

Authors: Mahmoud, Ahmed S., Mohamed, Nouran Y., Mostafa, Mohamed K., and Mahmoud, Mohamed S.

Effective Chromium Adsorption From Aqueous Solutions and Tannery Wastewater Using Bimetallic Fe/Cu Nanoparticles: Response Surface Methodology and Artificial Neural Network

Ahmed S. Mahmoud[1] (iD), Nouran Y. Mohamed[1],
Mohamed K. Mostafa[2] (iD) and Mohamed S. Mahmoud[1] (iD)

[1]Housing and Building National Research Center (HBRC), Egypt. [2]Badr University in Cairo (BUC), Egypt.

ABSTRACT: Tannery industrial effluent is one of the most difficult wastewater types since it contains a huge concentration of organic, oil, and chrome (Cr). This study successfully prepared and applied bimetallic Fe/Cu nanoparticles (Fe/Cu NPs) for chrome removal. In the beginning, the Fe/Cu NPs was equilibrated by pure aqueous chrome solution at different operating conditions (lab scale), then the nanomaterial was applied in semi full scale. The operating conditions indicated that Fe/Cu NPs was able to adsorb 68% and 33% of Cr for initial concentrations of 1 and 9 mg/L, respectively. The removal occurred at pH 3 using 0.6 g/L Fe/Cu dose, stirring rate 200 r/min, contact time 20 min, and constant temperature $20 \pm 2°C$. Adsorption isotherm proved that the Khan model is the most appropriate model for Cr removal using Fe/Cu NPs with the minimum error sum of 0.199. According to khan, the maximum uptakes was 20.5 mg/g Cr. Kinetic results proved that Pseudo Second Order mechanism with the least possible error of 0.098 indicated that the adsorption mechanism is chemisorption. Response surface methodology (RSM) equation was developed with a significant p-value = 0 to label the relations between Cr removal and different experimental parameters. Artificial neural networks (ANNs) were performed with a structure of 5-4-1 and the achieved results indicated that the effect of the dose is the most dominated variable for Cr removal. Application of Fe/Cu NPs in real tannery wastewater showed its ability to degrade and disinfect organic and biological contaminants in addition to chrome adsorption. The reduction in chemical oxygen demand (COD), biological oxygen demand (BOD), total suspended solids (TSS), total phosphorus (TP), total nitrogen (TN), Cr, hydrogen sulfide (H_2S), and oil reached 61.5%, 49.5%, 44.8%, 100%, 38.9%, 96.3%, 88.7%, and 29.4%, respectively.

KEYWORDS: adsorption, kinetics, response surface methodology, artificial neural network, tannery wastewater, chromium, bimetallic Fe/Cu nanoparticles

TYPE: Original Research

CORRESPONDING AUTHOR: Ahmed S. Mahmoud, Sanitary and Environmental Institute (SEI), Housing and Building National Research Center (HBRC), 87 Tahrir Street, Dokki, Giza, 1770, Egypt. Email: ahmeds197@gmail.com

Introduction

Wastewater generated from the tanning industry represents one of the major sources of environmental pollution since it contains many contaminants, such as heavy metals, chloride, total organic compounds (TOC) (Abdel-Aziz & Fayyadh, 2021). Represented in biological oxygen demand (BOD) and chemical oxygen demand (COD), toxic chemicals, lime with high suspended and dissolved salts, and other pollutants (Hamdy et al., 2019; Mohan et al., 2008; Mostafa & Peters, 2016; Saryel-Deen et al., 2017). Heavy metal pollution has a significant area of concern due to high concentrations released into the environment (Masindi & Muedi, 2018). chrome contamination is one of the worst types of pollutants that can cause different health problems and classified as carcinogenic material (Group A) in US-EPA (B. He et al., 2013; Z. Li et al., 2014; Lu et al., 2015). Chromate and dichromate salts are widely used for leather tanning, nuclear power plants and textile industries (Förstner & Wittmann, 2012; Garg et al., 2009; Nriagu, 1988). Chromium has several oxidation states divalent, trivalent, pentavalent, and hexavalent mainly found in tanning industries and the hexavalent chromium ion is the most dangerous material for plants, animals and humans (Agrawal, 2012; Annadhasan et al., 2019; Chiu et al., 1998). A high concentration of trivalent chromium may cause several diseases as allergic skin reactions (Langat, 2018) although the low concentration is necessary for plant and animal metabolism. Chromium can replace other metals in biological systems with toxic effects and its accumulation throughout the food chain leads to serious ecological and health problems (Jaishankar et al., 2014; Wuana & Okieimen, 2011).

Thus, it is necessary to get rid of chromium from wastewater before releasing it into the environment. Some kinds of literature have reported that more than 65% of used Cr salts react with leathers, while the Cr leftover remains in the effluent (Karabay, 2008; Kurniawan et al., 2011).

Several treatment technologies, like chemical precipitation, filtration, electrocoagulation, bioremediation, ion exchange, and adsorption, were tested to remove chromium from aqueous solutions and real wastewater (El-Shafei et al., 2016; Peng & Guo, 2020). Many research works have been recently published regarding the utilization of nanoparticles, especially nano Zero Valent Iron (nZVI), which is a promising material for the removal of chromium atoms from polluted water and wastewater due to its high surface area and reactivity (J. Li et al., 2020; Mystrioti et al., 2015). Loading nZVI with another catalytic metal, like palladium (Pd), nickel (Ni), and copper (Cu), can

provide more active sorbent sites and donate free electrons on nanoparticles' surface (Abdel-Aziz et al., 2020; Mahmoud, Ismail, et al., 2020; T. Zhou et al., 2010). New adsorption and degradation technique called a bimetallic system was developed to reinforce the reduction capability of nZVI with the rise of reaction potential by adding the zerovalent copper (Cu^0) (Abdel-Aziz et al., 2019; Stefaniuk et al., 2016). Few kinds of research have been conducted on chromium removal from real industrial wastewaters, especially tannery wastewater using nanosorbent.

Several sorbent materials were used to establish the best removal percentages for different chromium concentrations such as coconut tree sawdust, coconut tree sawdust, avocado kernel seeds (AKS), *Juniperus procera* sawdust (JPS), P. shell, C. F. leaves, sawdust, rice husk ash, red mud, modified groundnut hull, Ni/Fe bimetallic nanoparticles, maghemite NPs, bio prepared iron oxide nanoparticles, Fe_3O_4/activated carbon nanocomposite, Fe_3O_4 NPs, unsupported magnetite, and montmorillonite-supported magnetite nanoparticles were listed in Table 7. The best removal percentages were selected at the optimum operating conditions from, pH, dose, time, rate and initial concentrations, the optimum conditions were also placed in Table 7.

In this study, Fe/Cu NPs were prepared using chemical reduction in aqueous solutions through acidic conditions. The incorporation of copper with iron enhances the stability and adsorption behavior (Mahmoud, Ismail et al., 2020a). The prepared Fe/Cu nanoparticles were tested for the removal of Cr from both aqueous solutions and real tannery wastewater. The optimum conditions were obtained by addressing the effect of different operating parameters (Fe/Cu) nanoparticles dose, contact time, pH, initial Cr concentration, and stirring rate) on the Cr removal efficiency. Based on the obtained optimum conditions, the Fe/Cu nanoparticles were examined for the removal of different contaminants from real tannery wastewater, such as COD, TSS, BOD, total-nitrogen (TN), total phosphorus (TP), chromium (Cr), lead (Pb), copper (Cu), cadmium (Cd), boron (B), mercury (Hg), nickel (Ni), cyanide (CN), phenols, hydrogen sulfide (H_2S), oil, arsenic (As), and tin (Sn). The novelty of this study represented using Fe/Cu NPs for the first time in real tannery wastewater treatment.
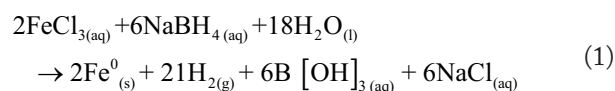
Materials and Methods

Chemicals and reagents

The following chemicals (Powder and solutions) were used in the current study: Ferric chloride ($FeCl_3.6H_2O$, 98.5% pure, Arabic Lab.), Sodium borohydride ($NaBH_4$, 98% pure, CDH Company), copper (II) sulfate pentahydrate ($CuSO_4.5H_2O$, 99.5%, WINLAB), Ethanol (C_2H_5OH 99%, World co. for sub & med industries), sulfuric acid (H_2SO_4, 95–97%, Honeywell Co.), sodium hydroxide (NaOH, 99% pure, Oxford Co.), and standard chrome solution, $Cr(NO_3)_3$, 998 ± 5 mg/L, Merck company.

Preparations and characterization of sorbent material

Preparations of nZVI. About 1.0812 g from ferric chloride ($FeCl_3.6H_2O$) was completely dissolved in 60 mL 4/1 (v/v) ethanol/ deionized water mixture. The reducing agent was prepared by dissolving exactly 0.7564 g $NaBH_4$ at 200 mL of deionized water. The reducing $NaBH_4$ solution was poured into a burette and slowly dropped into the $FeCl_3$ solution at a rate of 25 μL/s. The black precipitate immediately formed after the first drops of $NaBH_4$ solution as explained in Eq. 1. The chemical reduction between $NaBH_4$ and $FeCl_3$ was used to form black nZVI. The mixture was stirred for another 10 min after adding the excess amount of $NaBH_4$ to complete $FeCl_3$ reduction. Then, the normal filtration technique was applied to the separation and washing of nanoparticles from the aqueous solution. Finally, the prepared iron nanoparticles were dried at 80^0C for 3 hr. For the storage purpose, the prepared nZVI were protected against oxidation by adding a layer of acetone (Mahmoud, Mostafa, & Nasr, 2019)

$$2FeCl_{3(aq)} + 6NaBH_{4\,(aq)} + 18H_2O_{(l)}$$
$$\rightarrow 2Fe^0_{\,(s)} + 21H_{2(g)} + 6B\,[OH]_{3\,(aq)} + 6NaCl_{(aq)} \quad (1)$$

Preparation of bimetallic Fe/Cu. The nano Fe/Cu was prepared according to a study conducted by Zin et al. (2013). About 1 g from freshly prepared nZVI was added into copper sulfate ($CuSO_4.5H_2O$) solution at a flow rate of 0.1 g per 60 s with powerful stirring. $CuSO_4.5H_2O$ solution was prepared by mixing 0.1 g from CuSO4 with 100 mL ethanol/distilled water (DW) (1:1) at 60ºC. After that, the solution was allowed to settle for 15 min. The color of black nZVI was changed into coppery color. The solution was filtrated using two sheets of filter paper—Whatman- number 1 circle and diameter 150 mm. After filtration, the bimetallic Fe/Cu nanoparticles were washed two times with 20 mL of absolute ethanol (99.99%, HPLC grade). The prepared Fe/Cu NPs was dried in an oven at 60ºC for 5 hr. The prepared Fe/Cu NPs were stored under nitrogen and covered with a thin parafilm layer (Mahmoud, Mostafa, & Nasr, 2019).

Characterizations

The x-ray diffraction pattern (XRD) was used for investigating the material structure of the prepared bimetallic Fe/Cu nanoparticles (Mahmoud et al., 2018). A Philips XRG 3100 diffractometer (Netherlands) was used for performing the XRD analysis, where a graphite monochromator and a copper K-alpha radiation were utilized to generate x-rays with a wavelength of 1.5418 A^0 (Mahmoud, Farag, et al., 2019). The X-Ray was operated at a voltage of 40 kV and a current of 40 mA. After placing the prepared Fe/Cu NPs in a stainless-steel holder, the sample was scanned in a range from 5^0 to 70^0 and at a rate of 0.0167^0/s (Mahmoud et al., 2018, Mahmoud, Ismail, et al., 2020). The surface structure of the prepared Fe/Cu NPs

Table 1. Batch Experiments at Different Operating Parameters.

EFFECT	OPERATING PARAMETERS				
	DOSE (G)	CONTACT TIME (MIN)	PH	STIRRING RATE (R/MIN)	CONCENTRATION (MG/L)
pH	0.6	20	3–11	200	5
Bimetallic Fe/Cu dose	0.1–1	20	3	200	5
Contact time	0.6	10–50	3	200	5
Stirring rate	0.6	20	3	100–300	5
Initial Cr concentration	0.6	20	3	200	1–9

was also examined using scanning electron microscope (SEM) (Philips Quanta 250 FEG, USA). The SEM instrument was operated at a voltage of 20 KV and a magnification of 120,000x.

Experimental setup

The adsorption of chromium ions was equilibrated with Fe/Cu NPs by batch technique. The effect of different operating parameters from pH, bimetallic Fe/Cu dose, time, rate, and Cr initial concentration was listed in Table 1. A known weight of Fe/Cu NPs was equilibrated with 1000 mL of synthetic concentration of Cr in Erlenmeyer flasks and shacked at 150 r/min for 20 min. After equilibration, the solution was filtrated by Whatman filter paper No. 2, and the remained concentration was detected by atomic absorption spectroscopy (AAS) according to ASTM 2005 stander method for water and wastewater (Water Environment Federation, American Public Health Association, 2005). The removal percentages were calculated by equation (2). The amount of chrome sorbed by Fe/Cu NPs was calculated using equation (3)

$$Sorption\left(\%\right) = \left(\frac{C_0 - C_e}{C_0}\right) \times 100 \qquad (2)$$

where C_o is the initial chromium concentration in solution (mg/L) and C_e is the equilibrium concentration in solution (mg/L)

$$Q_e\left(mg/mg\right) = \frac{\left(C_0 - C_e\right)V}{m} \qquad (3)$$

where Q_e is the equilibrium adsorption capacity (mg/mg), m is the dry weight of the Fe/Cu NPs (mg), and V is the volume of aqueous solution (L)

The tannery wastewater samples were collected and tested to detect the initial chromium concentration, and the results were 8.2 and 2.73 for raw and secondary treated wastewater, respectively. Other wastewater contaminants were tested to make a comparison between them before, after different treatment processes and the allowable limits. At pH 3, stirring rate 200 r/min, contact time 20 min the effective dose was calculated to be 1.75 g/L. Samples and the selected dose were placed in Erlenmeyer flasks, shacked, filtrated, and measured to detect and compared the results as shown in Table 6.

Isotherm studies

The nonlinear adsorption model isotherms are equilibrated equations that are applied to conditions the adsorption process after the sorbent/adsorbate interaction for enough time to range the equilibrium process. The mathematical nonlinear equations of all implemented models. The Langmuir, Freundlich, Redlich–Peterson, Hill, Khan's model, Toth model, Sips, Koble–Corrigan, and Jovanovich adsorption isotherm models' descriptions with mathematical equations were placed in Supplementary material "Table S4."

Kinetic studies

The standard solutions were contacted with sorbent material until the equilibrium state during the period at a constant temperature. The quantity of sorbed chromium at time *t* is known Q*t* (mg/g), was calculated using equation (4)

$$Q_t = \frac{\left(C_o - C_t\right)V}{W} \qquad (4)$$

where "C_o" is the initial chromium concentration (mg/L), "C*t*" is the initial chromium concentration at time *t* (mg/L), "V" is the volume of the solution (L), and W is the weight of the sorbent (g).

Different kinetics models were tested to explore the suitable kinetic model which illustrates the kinetics of contaminants removal mechanism at different times. The pseudo-first-order (PFO) Proved that the bond between sorbate and sorbent is caused by hydrogen bonds and Van der Waals forces. The pseudo-second-order (PSO) assumes chemisorption reaction. Avrami model describes the solid transformation from the current phase to another phase at a constant temperature. Elovich's model describes the transfer of contaminants from the aqueous solution phase to the solid phase. Finally, the Intraparticle nonlinear model describes sorbent adsorbate transformation (Avrami, 1940; Fola et al., 2016; Ho & McKay, 1998a, 1999; Zeldowitsch, 1934b).

Validation of adsorption isotherms and kinetics

Five error function equations were selected to validate the best adsorption isotherm and kinetic models which describe the mechanism of removal (Mahmoud, Farag, & Elshfai, 2020). These error function equations include the Sum of the Squares of the Errors (ERRSQ), Marquardt's percent standard deviation (MPSD), Average Relative Error (ARE), a Composite Fractional Error Function (HYBRD), Chi error, and the Sum of the Absolute Errors (EABS) (Mahmoud, Farag, & Elshfai, 2020). Supplementary Table S1 includes an equation for each error function.

Neural network structure

An artificial intelligence neural network architecture was recognized to predict chromium removal efficiency. The ANN model involves input covariable (pH, Dose, time, stirring rate, and concentration), hidden layers (weight and bias), and the output layer or dependent layer (removal %). The structure of ANN was expressed as $5 - 4 - 1$ as shown in Supplementary Figure 1. The collected data from the five covariables are transferred into the input layer and divided into standard values for testing, training, and validation. The network name is "Multilayer perceptron (MLP)." The MLP model uses a feedforward backpropagation style and can have multiple hidden layers (in this case four hidden layers). It is one of the most regularly used ANN techniques for water and wastewater treatment (Mahmoud, Farag, & Elshfai, 2020; Mahmoud, Farag, et al., 2019).

Response surface methodology

The RSM regression statistical model shows a simultaneous confidence band for the fitted response surface. A diagram was designed to demonstrating a contour of RSM for best chromium removal. The independent covariables were pH, dose, time, rate of stirring, and concentration. The linear regression analysis was working to describe the RSM relation plots by using the experimental data

$$Y = \beta_0 + \beta_1 x_1 + \beta_2 x_2 + \beta_3 x_3 + \beta_4 x_4 + \beta_5 x_5 + \beta_6 x_6 \qquad (5)$$

where, Y is the predicted percentages response of chromium removal efficiency (%), x_1 is pH (3–11), x_2 is adsorbent dose (0.1–1.0 g), x_3 is stirring rate (100–300 RPM), x_4 is time (10–50 min), x_5 is initial chromium concentration (1–9 mg/L), β0 is the model intercept, and β_1, β_2, β_3, β_4, and β_5 are the linear coefficients of x_1, x_2, x_3, x_4, and x_5, respectively.

Results and Discussion

Characterization of Fe/Cu NPs

Figure 1(a) shows The XRD pattern for prepared pure nZVI with two peaks at $2\theta = 44.6°$ and $64.99°$ for planes Fe (110) and Fe (200), respectively. A sharp peak at $2\theta = 44.6°$ indicated domination of zero-valent iron (Fe^0) in the prepared sample.

The maximum half-peak width (FWHM) for $2\theta = 44.58$ and $64.99°$ was 0.0067 and 0.002898 radian, respectively indicated the formation of nano iron with an average size of 26 nm ± 3 nm. Figure 1(b) shows the XRD pattern for Fe/Cu nanoparticles with (2θ) from 5–70 indicated the formation of Fe/Cu NPs by three fundamental peaks at 2θ 43.3° for Cu, 44.7° for Fe, and 50.8° for Cu (Lucas et al., 2002; Omar, 2016). Figure 1(c) shows an SEM image of the synthesized bimetallic Fe/Cu nanoparticles. The SEM results indicated the formation of Fe/Cu NPs crystals with sizes 22.93, 19.23, 8.598, and 39.51 nm. The average Fe/Cu NPs size was 22.57 ± 11.1 nm. Figure 1(d) shows Energy-dispersive X-ray spectroscopy (EDAX) analysis for the selected nanoparticles 22.9 nm shows the formation of iron as the main peak, copper, outer oxide, and carbon layers.

Several nano-sorbents were used for the wastewater treatment process. Shape-dependent properties including size and reactivity are the main criteria for the reactivity of nanoparticles toward different contaminant removal. Yuan et al. (2009) studied the effect of size magnetite nanoparticles with size 25 nm for Cr(VI) and the obtained results indicated that the maximum Cr(VI) uptake about 18 mg/g throughout the Physicochemical interaction mechanism (Yuan et al., 2010). S. Zhou et al. (2014) studied the effect of Ni/Fe bimetallic nanoparticles on Cr(VI) removal with an average size of 30–60 nm. The maximum uptake was about 21 mg/g via both mechanisms adsorption/reduction process indicating the other metal facilitates the flow of electron transfer which can increase the reactivity of nano bimetallic (S. Zhou et al., 2014).

Effect of operating conditions

Effect of pH. The pH measurements of the aqueous solution are one of the most effective operating conditions in Cr removal. The pH can affect species distribution and the rate of Cr removal. The effect of pH on Cr removal efficiency was studied under the following operating conditions (Fe/Cu NPs dosage = 0.6 g/L, Cr initial conc.= 5 mg/L, contact time = 20 min, and stirring rate = 200 r/min). As illustrated in Figure 2(a), the Cr removal efficiency reached its maximum at pH 3 reaching 53%. With an increase in pH into neutral and alkaline medium, the removal efficiency decreased to 50% at pH 5.0% and 44% at pH 7. However, the removal efficiency increased to 48% at pH 11. This is maybe attributed to the alkaline conditions, where the OH^- in the solution can react with iron to produce an iron oxide passivation layer covering the surface of the nanoparticles, occupying the particle surface active sites and inhibiting the reduction reaction (Y. He et al., 2018; Mostafa et al., 2017). This suggested that acidic conditions are more favorable for Cr removal by Fe/Cu nanoparticles. It could be because the H^+ in the solution can dissolve the iron oxide film formed on the surface of the nanoparticles, which increased the exposure of the particle surface active site, thus improving the removal efficiency of Cr (Guan et al., 2015). Considering the removal efficiency and
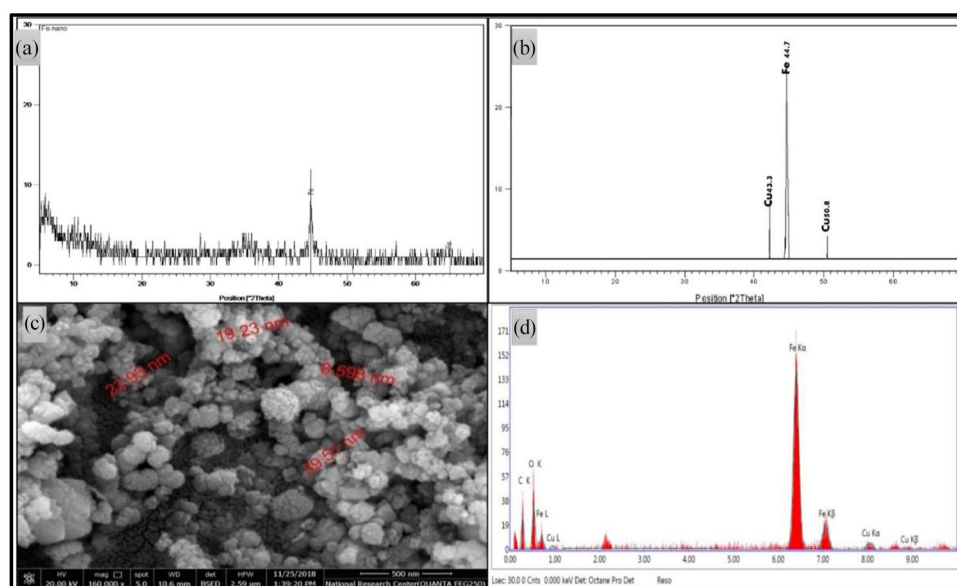
Figure 1. (a) XRD result of nZVI, (b) XRD of Fe/Cu NPs, (c) SEM of Fe/Cu NPs, and (d) EDAX of Fe/Cu NPs.
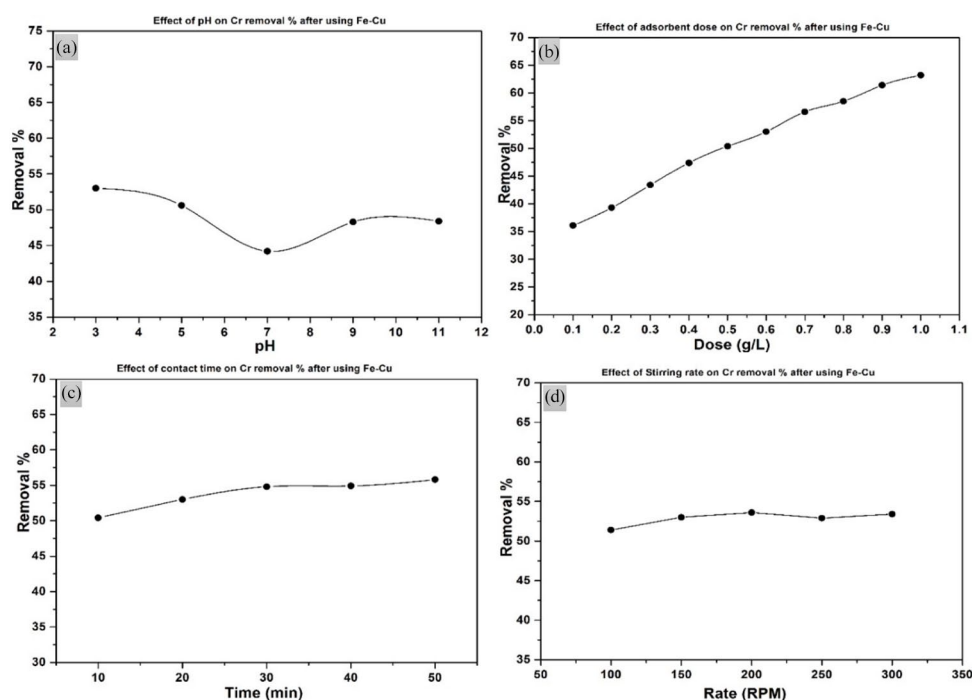
Figure 2. Effects of experimental factors on Cr removal of efficiency using Fe/Cu NPs: (a) pH, (b) dosage, (c) contact time, and (d) stirring rate.

the feasibility of actual operation, an initial pH of 3.0 was used as the optimum pH in this experiment. Lv et al. (2012) have tested the efficiency of highly active (nZVI)–Fe_3O_4 nanocomposites on the chromium (VI) removal, and the optimal pH for the removal of Cr was also reported as pH 3.

Effect of adsorbent dose. The effect of different adsorbent doses of Fe/Cu bimetallic nanoparticles on the Cr removal efficiency was studied under the following operating conditions (pH = 3, contact time = 20 min, Cr initial conc.= 5 mg/L, and stirring rate = 200 r/min). As illustrated in Figure 2(b), an increase in

the adsorbent dosage from 0.1 to 1 g/L resulted in an increase in the removal efficiency from 49% to 63% for 5 mg/L of Cr. The increase in the adsorption behavior is related to the increase in the availability of active sites on the bimetallic nanoparticles, in addition to the free electrons for the degradation process (Mahmoud, 2017). Mutongo et al. (2014) studied the aqueous Cr(VI) adsorption by using powder of potato peelings as a low-cost sorbent, and the achieved results indicated that Cr(VI) removal efficiency from the solution increased steadily with the increase in the absorbent dose (Mutongo et al., 2014). Low et al. (2001) have test quaternized wood as sorbent for

hexavalent chromium, and the achieved results indicated that by increasing the sorbent dosage, the percentage uptake increased which agrees with the obtained results (Low et al., 2001).

Effect of contact time. The effect of contact time on the Cr removal efficiency was studied under the following operating conditions (pH = 3, Fe/Cu NPs dose = 0.6 g/L, Cr initial conc. = 5 mg/L and stirring rate = 200 r/min). As indicated in Figure 2(c), the Cr adsorption efficiency has increased with the increase in contact time until reaching the equilibrium state after 30 min. The rapid increase in the chromium adsorption efficiency at the beginning of the reaction is mainly attributed to the existence of enormous vacant active sites in the adsorbent surface. However, by increasing the time the validity of vacant sites on Fe/Cu NPs surface become limited, which makes the adsorption efficiency reach the equilibrium state. Garg et al. (2009) have studied the effect of using banana peel as a green sorbent for removal of Cr(VI) from industrial wastewater. They have achieved Cr(VI) removal efficiency of 95% at the following optimum conditions: contact time 10 min, pH 2, and stirring rate 100 r/min. Another study indicated that the effective time to remove 50 mg/L of chrome using modified sugarcane bagasse at pH 2 and stirring rate 250 r/min was 60 min (Garg et al., 2009).

Effect of stirring rate. The effect of rate on the chromium removal efficiency was studied under the following operating conditions (pH = 3, Fe/Cu NPs dose = 0.6 g/L, Cr initial conc. = 5 mg/L, and contact time = 20 min). The effect of agitation speed on Cr removal efficiency was examined in the range of 100–300 r/min. As illustrated in Figure 2(d), the results revealed that the Cr removal efficiency remains constant beyond the agitation speed of 150 r/min. Weng et al. (2009) reported that this phenomenon can be attributed to the little resistance of the boundary layer and high mobility of the system. Hence, the agitation speed of 150 r/min was selected as the optimal mixing speed in this study. Two types of adsorption occur in nZVI surfaces; physical and chemical adsorption (Boparai et al., 2011). Chemical adsorption depends on the charge between the absorbed molecule and sorbent charge (Farag et al., 2018). Physical adsorption depends on vacant sites on the surface by Van der Waals force. Chemical adsorption is more stable than physical adsorption and mainly the stirring rate effect cannot decrease its stability—covalent bond—(Graham, 1953; Ho & McKay, 1998; Lin & Dufresne, 2013). The amount of adsorbed molecules in physical adsorption equals the summation of adsorbed materials for all individual active sites (Gilliland et al., 1974; Meyers & Liapis, 1999). The adsorption technique depends on binding energy between adsorbed molecules and sorbents. The adsorption energy decreased gradually until vanishes with the complete adsorption process (Zeldowitsch, 1934a). So, the little increase in the removal efficiency due to stirring rate is relative to

chemisorption reaction and this agrees with the kinetic data (Ho & McKay, 1999).

Effect of initial concentration. The effect of initial chromium concentration on the removal efficiency was studied under the following operating conditions (pH = 3, Fe/Cu NPs dose = 0.6 g/L, stirring rate = 200 r/min, and contact time = 20 min). In this study, the removal of Cr was investigated at initial Cr concentrations of 1, 3, 5, 7, and 9 mg/L. As shown in Figure 3(a), the Cr removal efficiency reached 68% at an initial concentration of 1 mg/L. Then, the removal efficiency decreased to 53%, 42%, and 33% at an initial Cr concentration of 5, 7, and 9 mg/L, respectively. In addition, it has been noticed that the amount of Cr uptake increased with the increase in the initial Cr concentration to reach a maximum uptake at concentration of 5 mg/L. This phenomenon may be attributed to the rise in the concentration gradient, which agrees with the results reported by Luo et al. (2013).

Adsorption studies

As shown in Table 2, Khan Model has the lowest summation of errors of 0.199. Khan's model describes the adsorption process for pure solutions and identifies the maximum uptake of the adsorbent into the solution. According to Khan Model, the maximum uptake is 20.54 mg/g. Supplementary Table 2 shows the results of the experimental and calculated Q_e (mg/g) for all nonlinear isotherm models after using Fe/Cu NPs. The adsorption isotherm for adsorption of chrome onto Fe/Cu NPs indicated that Khan Model is the most preferred model which better describes the adsorption process.

Kinetics studies

Figure 4 describes the nonlinear relations between different kinetic models and Supplementary Table 3 shows the results of the experimental and calculated Q_t (mg/g) for all nonlinear kinetic models after using Fe/Cu NPs. The kinetic isotherms were solved a nonlinear equation of PFO, PSO, Elovich Model, Avrami, and Intraparticle kinetic models. The achieved results indicated that the kinetic data is a better fit than the PSO model, with the lowest summation of errors equal to 0.098 (Table 3). PSO kinetic mechanism indicated that the desorption of chrome onto Fe/Cu NPs is dependent on concentration and dose together, and the adsorption mechanism is chemically rated controlling. Also, electrons are covalently exchanged or shared between sorbate and sorbent, meaning that the reaction is chemisorptions (Ho & McKay, 1999).

Artificial intelligence

Artificial neural network (ANN) was trained using the back-propagation algorithm using sample training 76.7% and testing
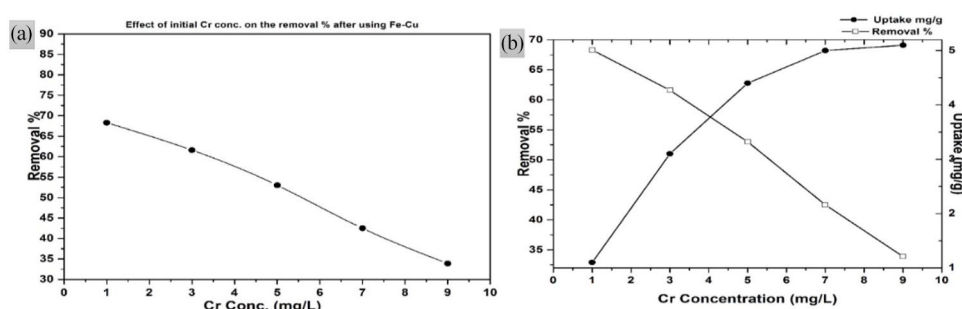
Figure 3. Effects of experimental factors on Cr removal of efficiency using Fe/Cu NPs: (a) Cr initial concentration and (b) uptake/removal% relation.

Table 2. Results of Isotherm Models After Using Fe/Cu NPs for Chromium Removal.

	REDLICH-PETERSON		HILL		SIPS		KHAN		TOTH	
Constants	Kr	3.44	QH	5.45	Qs	5.45	Qk	20.54	Kt	2.48
	Br	0.77	nH	1.36	Ks	1.10	Bk	0.20	at	1.16
	G	1.15	KD	0.88	Bs	1.36	Ak	2.04	t	2.48
ERRORS										
Chi error	1.005		0.119		0.119		0.002		0.063	
ERRSQ	0.009		0.064		0.064		0.007		0.185	
HYBRD	0.005		0.019		0.019		0.002		0.068	
MPSD	0.003		0.007		0.007		00.001		0.039	
ARE	0.083		0.177		0.177		0.037		0.326	
EABS	0.174		0.542		0.542		0.152		0.863	
Error sum	1.278		0.928		0.928		0.199		1.543	
	KOBLE–CORRIGAN		JAVANOVIC		FREUNDLICH		LANGMUIR			
Constants	A	6.22	Q_m	5.05	Kf	2.74	Q_0	6.17		
	B	1.14	Kj	0.82	n	2.61	b	0.86		
	D	1.36								
ERRORS										
Chi error	0.019		0.006		0.393		0.063			
ERRSQ	0.064		0.021		1.104		0.185			
HYBRD	0.019		0.006		0.511		0.068			
MPSD	0.007		0.002		0.350		0.039			
ARE	0.177		0.090		0.894		0.326			
EABS	0.542		0.292		2.115		0.863			
Error sum	0.828		0.416		5.368		1.543			

NPs: nanoparticles; ERRSQ: Sum of the Squares of the Errors; HYBRD: Composite Fractional Error Function; MPSD: Marquardt's percent standard deviation; ARE: Average Relative Error; EABS: Sum of the Absolute Errors.

23.3% for 30 valid results with a total number of 30 runs. The network trained by making a continuous process connection between weight and bias in which the network is implanted as shown in Supplementary Figure 1 with Rescaling Method for Covariates Standardized test, activation Function-Hyperbolic tangent-test, the sum of squares error was 0.042 and relative error 0.022. Results showed that there was a small deviation between the predictive values and normalized values as shown in Figure 5. Also, there was a small deviation between the residual value and predictive value (-0.4, +0.2%) indicating the reality of the result and the effectivity of model results to label the relation between chrome removal efficiency and other variables. Figure 6 shows the sensitivity analysis results which indicated that the Fe/Cu NPs dose is the most effective parameter with
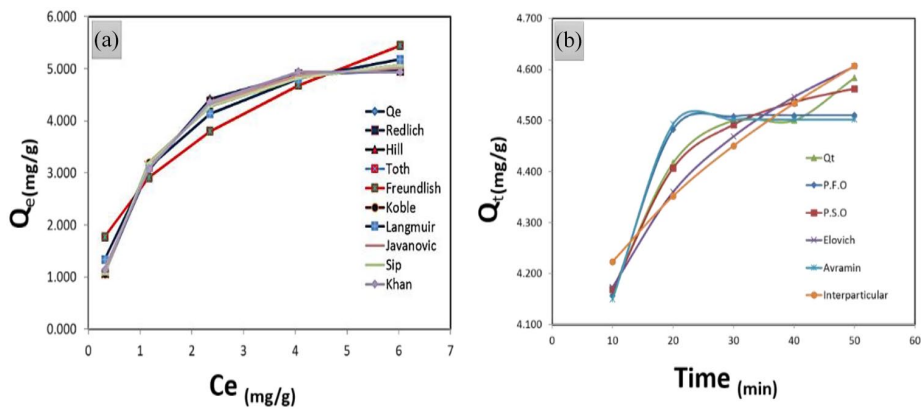
Figure 4. (a) Adsorption isotherm, and (b) kinetic models for chrome removal using bimetallic Fe/Cu NPs.

Table 3. Results of Different Kinetic Models After Using Bimetallic Fe/Cu Nanoparticles for Chrome Removal.

	P.F.O	P.S.O	ELOVICH	AVRAMI	INTRAPARTICLE
Constants	$Q_e = 4.510$ $K_1 = 0.255$	$Q_e = 4.672$ $K_2 = 0.177$	$\alpha = 14.2E4$ $\beta = 3.722$	$Q_e = 4.502$ $K_{av} = 0.133$ $N_{av} = 1.283$	$K_{id} = 0.098$ $C_i = 3.913$
ERRORS					
Chi error	0.002	00.001	0.002	0.003	0.003
ERRSQ	0.010	0.002	0.007	0.013	0.012
HYBRD	0.002	00.001	0.002	0.003	0.003
MPSD	00.001	00.001	00.001	0.001	0.001
ARE	0.037	0.017	0.037	0.040	0.052
EABS	0.167	0.078	0.164	0.177	0.228
Error sum	0.219	0.098	0.211	0.236	0.298

PFO: pseudo-first-order; PSO: pseudo-second-order; ERRSQ: Sum of the Squares of the Errors; HYBRD: Composite Fractional Error Function; MPSD: Marquardt's percent standard deviation; ARE: Average Relative Error; EABS: Sum of the Absolute Errors.
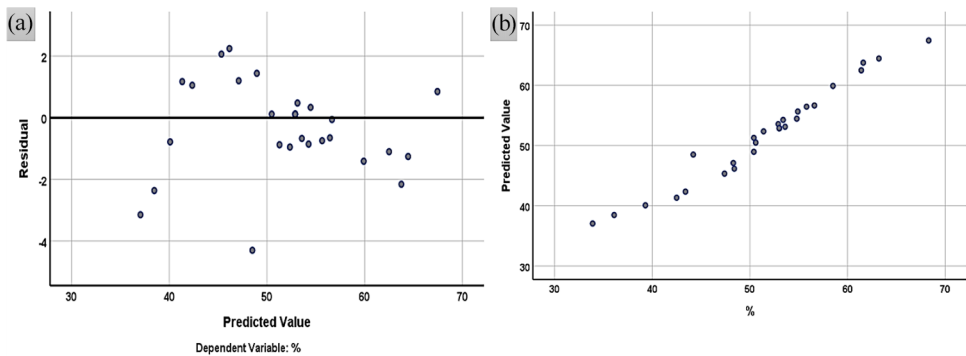
Figure 5. (a) ANN relation between residual and predicted removal %, and (b) ANN relation betweem predicted and true removal % for chrome removal using bimetallic Fe/Cu NPs.

normalized importance of 100% followed by initial concentration 82.3%, pH 29.5%, stirring rate 16.4%, and finally contact time 14.5%.

Response surface methodology (RSM)

Linear regression statistical equations (General Linear Model [GLM]) were estimated for chrome removal as a dependent parameter with pH, dose, stirring rate, contact time, and concentrations as Predictors by using Enter methods (Mahmoud, Farag, et al., 2019; Edwards, 2002; Edwards & Parry, 1993; Larson-Hall, 2015) with R^2 98.6% and Std. The error of Estimate 1.4. The achieved results indicated that the model was significant (p-value $< .05$) to describe the relationship between the chrome removal efficiency and other studied variables, as shown in Table 4. The results indicated that pH, dose,

Figure 6. ANN importance and normalized importance result for chrome removal using bimetallic Fe/Cu NPs.

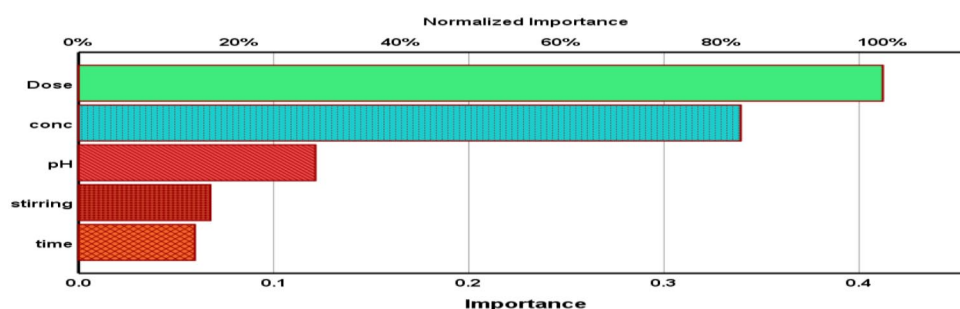**Table 4.** ANOVA Analysis for "Chromium Removal as Dependent Variable" and "Predictors."

ANOVAª		SUM OF SQUARES	DF	MEAN SQUARE	F	SIG.
MODEL						
1	Regression	1643.654	5	328.731	163.751	.000ᵇ
	Residual	48.180	24	2.007		
	Total	1691.834	29			

ANOVA: analysis of variance.
ªDependent variable: chrome removal.
ᵇPredictors: (Constant), pH, dose, time, stirring rate and concentration.

Table 5. The B Statistics, t-Value and p-Value for Case Study Variables and Chrome Removal.

COEFFICIENTSª		UNSTANDARDIZED COEFFICIENTS		STANDARDIZED COEFFICIENTS	*T*	SIG.
MODEL		B	STD. ERROR	BETA		
1	(Constant)	54.097	2.165		24.993	.000
	pH	−.749	.138	−.188	−5.416	.000
	Dose (mg/L)	30.439	1.547	.679	19.682	.000
	Stirring Rate (RPM)	.009	.008	.043	1.226	.232
	Min	.136	.038	.124	3.584	.001
	mg/L	−4.395	.224	−.676	−19.618	.000

ªDependent variable: Bulimia Nervosa.

contact time, and concentrations were significant variable (p-value $<$ .05) for chrome removal, while the stirring rate effect was not a significant variable (p-value $>$ .05) for chrome removal as shown in Table 5. Figure 7(a) describes GLM relations between expected and observed "Cr" removal percentages using all variables showing small deviations between the observed and expected results. Figure 7(b) shows the standardized residual between results showing estimated residual values between (-3 and +3%) from removal percentages for all results and the most frequent results were between (+1 and -1%) showing agreement with the estimated ANN results.

Equation (6) shows all-regression models (significant and insignificant). For simplicity, the insignificant factors were excluded, and a new regression model was obtained (equation [7])

$$Y = 54.097 - 749x_1 + 30.439x_2 + 0.009x_3 + 0.136x_4 - 4.395x_5 \quad (6)$$

$$Y = 54.097 - 749x_1 + 30.439x_2 + 0.136x_4 - 4.395x_5 \quad (7)$$

where, Y is the predicted response of different wastewater contaminants removal efficiency (%), x_1 is pH (3–11), x_2 is Fe/Cu NPs dose (0.1–1.0 g), x_3 is rate (100–300 r/min), x_4 is time (10–50 min), x_5 is initial Cr concentration (1–9 mg/L), β0 is the model intercept, and β_1, β_2, β_3, β_4, and β_5 are the linear coefficients of x_1, x_2, x_3, x_4, and x_5, respectively.
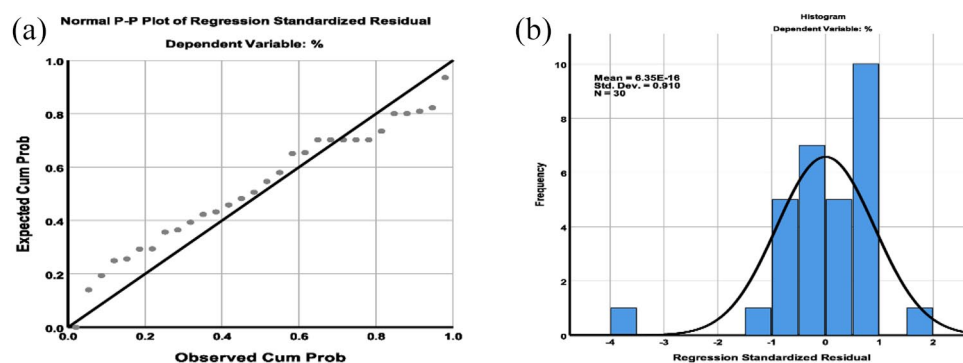
Figure 7. (a) P-P plot regression plot, and (b) residual histogram for chrome removal using bimetallic Fe/Cu NPs.

Table 6. Characteristics of Real Tannery Wastewater and Corresponding Removal Efficiencies.

PARAMETER	UNIT	RAW WASTEWATER	SECONDARY TREATED WASTEWATER	FE/CU NPS + SEDIMENTATION + PH ADJUSTMENT	LIMITS: LAW 93/1962[a]
pH	—	9.83	6.7	6.1	6–9.5
Chemical oxygen demand (COD)	mg/L	9540	2470	950	1100
Biological oxygen demand (BOD)	mg/L	5693	1010	510	600
Total suspended solids (TSS)	mg/L	6222	1150	635	800
Total phosphorus (TP)	mg/L	1.7	0.9	0	25
Total nitrogen (TN)	mg/L	69.3	55.2	33.7	100
Oil	mg/L	2.3	1.7	1.2	100
Hydrogen sulfide (H_2S)	mg/L	48.9	23.9	2.7	10
CN	mg/L	0.012	0	0	0.2
Phenols	mg/L	0	0	0	0.05
Cadmium (Cd)	mg/L	0	0	0	0.2
Lead (Pb)	mg/L	0.001	0	0	1
Copper (Cu)	mg/L	0	0	0	1.5
Nickel (Ni)	mg/L	0.009	0	0	1
Arsenic (As)	mg/L	0.003	0	0	2
Chromium (Cr)	mg/L	8.2	2.73	0.1	0.2
Mercury (Hg)	mg/L	0	0	0	0.2
Tin (Sn)	mg/L	0	0	0	2
Boron (B)	mg/L	0	0	0	1
Deposits after 10 min	cm^3	75	7	3	8
Deposits after 30 min	cm^3	42	17	5	15

NPs: nanoparticles.
[a]Limits 93/1962: discharge of wastewaters to public sewers.

Removal of chromium and other contaminants from tannery wastewater

The third column in Table 6 represents the characteristics of the raw tannery wastewater, while the fourth column represents the characteristics of the wastewater after subjecting to secondary treatment. The concentration of most of the tested parameters has exceeded the allowable limits specified in law 93/1962 for discharging treated wastewater to the public sewers. In this study, the efficiency of the prepared bimetallic Fe/Cu NPs was applied as a tertiary treatment for the treatment of secondary treated tannery wastewater. The most efficient Fe/Cu NPs dose of 1.75 g/L was estimated using the obtained RSM equation No. 6 to reach 100% removal of Cr. Regarding the other variables, the optimum conditions were obtained from the batch

experiments conducted in this study: pH 3, stirring rate 200 r/min, contact time 20 min. The pH was adjusted using sodium hydroxide and sulfuric acid. The results showed a significant decrease in COD (61.5%), BOD (49.5%), TSS (44.8%), TP (100%), TN (38.9%), Cr (96.3%), H_2S (88.7%), and oil (29.4%). The results also showed that the concentration of all tested parameters did not exceed the allowable limits specified in law 93/1962. A zero concentration was also reported for some parameters at the treated effluent, such as Cu, Cd, Sn, Hg, and B (Table 6), which confirms the safety use of Fe/Cu NPs in wastewater treatment. As illustrated in Table 6, the suspended solids deposits after 10 and 30 min did not exceed the limits specified in law 93/1962. Egyptian and international standards for discharging to different sources were placed in Supplementary material Table S5.

Based on the obtained results, the Fe/Cu NPs with the selected ratio proved the ability to degrade and adsorb a wide range of wastewater contaminants especially COD, BOD, TSS, and heavy metals. So, it is necessary to specify the removal conditions and limitations on future works.

Adsorption of chromium by various adsorbents

Table 7 summarizes the removal efficiencies of Cr using various adsorbents. The Fe/Cu NPS used in this study exhibited a lower removal performance than the other adsorbent materials listed in Table 7. This is mainly due to the low adsorbent dose applied in this study (only 0.6 g/L) compared to the other adsorbents listed in the table, such as Coconut tree sawdust, Papaya peels (PP), avocado kernel seeds (AKS), Juniperus procera, sawdust, P. Shell, C. F. Leaves, and rice husk ash, where the adsorbent dose ranging from 10 to 16.6 g/L. However, the Fe/Cu NPS exhibited a higher removal performance than the other adsorbents when it is applied for tannery wastewater treatment and the dose increased to 1.75 g/L. In addition, the Fe/Cu NPS achieved an enhanced removal efficiency at a lower contact time compared to the other adsorbents. Generally, there are a big variation in the Cr removal efficiencies using different adsorbents, and this is mainly due to the variation in the experimental conditions (e.g., adsorbent dosage, initial Cr concentration, pH, contact time, stirring rate, etc.).

Conclusion

This study showed that the bimetallic Fe/Cu NPs were efficient in the removal of Cr from aqueous solutions, achieving a maximum removal efficiency of 68% at an initial concentration of 1 mg/L, pH 3 using 0.6 g/L Fe/Cu dose, stirring rate 200 r/min, and contact time 20 min. The isotherm study indicated that the adsorption data for Fe/Cu NPs are in good agreement with Khan Model, while the kinetic study indicated that the PSO model best describes the data. These findings showed that the desorption of chrome onto Fe/Cu NPs is dependent on concentration and dose together, and the

Table 7. Adsorption of Chromium Using Various Adsorbents.

ADSORBENT	EXPERIMENTAL FACTOR					CHROMIUM REMOVAL EFFICIENCY	REFERENCES
	PH	ADSORBENT DOSAGE, G/L	STIRRING RATE, R/MIN	INITIAL CHROMIUM CONCENTRATION	CONTACT TIME, MINUTE		
Coconut tree sawdust	3	1–15	150	5–20 mg/L	180	98.84% for 5 mg/L 84.06% for 20 mg/L	Selvi et al. (2001)
Papaya peels (PP)	1	16.66	200	10 mg/L	180	99%	Mekonnen et al. (2015)
Avocado kernel seeds (AKS)	1	16.66	200	10 mg/L	180	97%	Mekonnen et al. (2015)
Juniperus procera sawdust (JPS)	1	16.66	200	10 mg/L	180	95%	Mekonnen et al. (2015)
P. Shell	2	10.0	130	40 mg/L	360	100%	Ahmad et al. (2017)
C. F. Leaves	2	10.0	130	40 mg/L	360	98%	Ahmad et al. (2017)
Sawdust	2	10.0	130	40 mg/L	360	98%	Ahmad et al. (2017)

(Continued)

Table 7. (Continued)

ADSORBENT	EXPERIMENTAL FACTOR					CHROMIUM REMOVAL EFFICIENCY	REFERENCES
	PH	ADSORBENT DOSAGE, G/L	STIRRING RATE, R/MIN	INITIAL CHROMIUM CONCENTRATION	CONTACT TIME, MINUTE		
Rice husk ash	3	10.0	NA	50 mg/L	240	94.8%	Bhattacharya et al. (2008)
Sawdust	3	10.0	NA	50 mg/L	240	86.5%	Bhattacharya et al. (2008)
Sawdust	2	16.0	100	100 mg/L	120	81%	Dakiky et al. (2002)
Red mud	5.2	0.1	NA	10 mg/L	120	95%	Pradhan et al. (1999)
Modified groundnut hull	2	0.2	125	13 mg/L	120	90%	Owalude & Tella (2016)
Ni/Fe bimetallic nanoparticles	3	1.0	200	25 mg/L	150	90%	S. Zhou et al. (2014)
nanoscale maghemite	2.5	5.0	NA	50 mg/L	15	90%	Hu et al. (2005)
iron oxide nanoparticles	3	2.5	120	10 mg/L	120	99%	Chatterjee et al. (2020)
Fe_3O_4/activated carbon nanocomposite	2	5	180	50 mg/L	15	95.3%	Jain et al. (2018)
Fe_3O_4	2	5	180	50 mg/L	60	75%	
unsupported magnetite	1	1	160	10.6 mg/L	10	100%	Yuan et al. (2009)
Montmorillonite-supported magnetite nanoparticles	1	1	160	15.3 mg/	10	100%	
Fe/Cu NPS	3	0.6	150	5 mg/L	20	53%	Current study
Fe/Cu NPS	3	1.75	150	2.73 mg/L Cr from real tannery wastewater	20	96.3%	Current study

NA: not available; NPs: nanoparticles.

adsorption mechanism is chemically rated controlling. The RSM with an r^2-value higher than .98 was found to be reliable in predicting Cr removal efficiency at different operating parameters. The ANN has also indicated that the adsorbent dose is the most dominated variable for Cr removal. These modeling techniques can assist in maximizing the performance of Fe/Cu NPs for treating wastewater contaminated by chromium under different operating conditions. The Fe/Cu NPs were able to treat secondary treated tannery wastewater, where the concentrations of COD, BOD, TSS, TP, TN, Cr, H_2S, and oil have decreased by about 61.5%, 49.5%, 44.8%, 100%, 38.9%, 96.3%, 88.7%, and 29.4%, respectively.

Declaration of Conflicting Interests

Funding

ORCID iDs

Ahmed S. Mahmoud (iD) https://orcid.org/0000-0003-3092-8056

Mohamed K. Mostafa (iD) https://orcid.org/0000-0001-9960-3474

Mohamed S. Mahmoud (iD) https://orcid.org/0000-0002-7224-6232

Supplemental Material

Supplemental material for this article is available online.

REFERENCES

Abdel-Aziz, H. M., Farag, R. S., & Abdel-Gawad, S. A. (2019). Carbamazepine removal from aqueous solution by green synthesis zero-valent iron/Cu nanoparticles with Ficus benjamina leaves' extract. *International Journal of Environmental Research*, 13(5), 843–852.

Abdel-Aziz, H. M., Farag, R. S., & Abdel-Gawad, S. A. (2020). Removal of caffeine from aqueous solution by green approach using Ficus benjamina zero-valent iron/copper nanoparticles. *Adsorption Science & Technology*, 38(9–10), 325–343.

Abdel-Aziz, H. M., & Fayyadh, S. N. (2021). Removal of Orange G by the Fenton process and Ficus benjamina nano-zerovalent iron. *Journal of Environmental Engineering and Science*, 40, 1–8.

Agrawal, A. (2012). Toxicity and fate of heavy metals with particular reference to developing foetus. *Advances in Life Sciences*, 2(2), 29–38.

Ahmad, A., Ghazi, Z. A., Saeed, M., Ilyas, M., Ahmad, R., Khattak, A. M., & Iqbal, A. (2017). A comparative study of the removal of Cr (VI) from synthetic solution using natural biosorbents. *New Journal of Chemistry*, 41(19), 10799–10807.

Annadhasan, M., Kasthuri, J., & Rajendiran, N. (2019). A facile sunlight-induced synthesis of phenylalanine-conjugated cholic acid-stabilized silver and gold nanoparticles for colorimetric detection of toxic Hg2+, Cr6+ and Pb2+ ions. *ChemistrySelect*, 4(21), 6557–6567.

Avrami, M. (1940). Kinetics of phase change. II transformation-time relations for random distribution of nuclei. *The Journal of Chemical Physics*, 8(2), 212–224.

Bhattacharya, A., Naiya, T., Mandal, S., & Das, S. (2008). Adsorption, kinetics and equilibrium studies on removal of Cr (VI) from aqueous solutions using different low-cost adsorbents. *Chemical Engineering Journal*, 137(3), 529–541.

Boparai, H. K., Joseph, M., & O'Carroll, D. M. (2011). Kinetics and thermodynamics of cadmium ion removal by adsorption onto nano zerovalent iron particles. *Journal of Hazardous Materials*, 186(1), 458–465.

Chatterjee, S., Mahanty, S., Das, P., Chaudhuri, P., & Das, S. (2020). Biofabrication of iron oxide nanoparticles using manglicolous fungus Aspergillus niger BSC-1 and removal of Cr (VI) from aqueous solution. *Chemical Engineering Journal*, 385, 123790.

Chiu, A., Chiu, N., Shi, X., Beaubier, J., & Dalai, N. (1998). Activation of a procarcinogen by reduction: Cr6+→ Cr5+→ Cr4+→ Cr3+ a case study by electron spin resonance (ESR/PMR). *Journal of Environmental Science & Health Part C*, 16(2), 135–148.

Dakiky, M., Khamis, M., Manassra, A., & Mer'Eb, M. (2002). Selective adsorption of chromium (VI) in industrial wastewater using low-cost abundantly available adsorbents. *Advances in Environmental Research*, 6(4), 533–540.

Edwards, J. R. (2002). Alternatives to difference scores: Polynomial regression and response surface methodology. In F. Drasgow & N. W. Schmitt (Eds.), *Advances in measurement and data analysis* (pp. 350–400). Jossey-Bass.

Edwards, J. R., & Parry, M. E. (1993). On the use of polynomial regression equations as an alternative to difference scores in organizational research. *Academy of Management Journal*, 36(6), 1577–1613.

El-Shafei, M., Mahmoud, A., Mostafa, M., & Peters, R. (2016, November 14–16). *Effects of entrapped nZVI in alginate polymer on BTEX removal* [Paper presentation]. The AIChE Annual Meeting, San Francisco, CA, United States.

Farag, R. S., Elshfai, M. M., & Mahmoud, A. S. (2018). Adsorption and kinetic studies using nano zero valent iron (nZVI) in the removal of chemical oxygen demand from aqueous solution with response surface methodology and artificial neural network approach. *Journal of Environment & Biotechnology Research*, 7(2), 12–22.

Fola, A. T., Idowu, A. A., & Adetutu, A. (2016). Removal of Cu2+ from aqueous solution by adsorption onto quail eggshell: Kinetic and isothermal studies. *Journal of Environment & Biotechnology Research*, 5(1), 1–9.

Förstner, U., & Wittmann, G. T. (2012). *Metal pollution in the aquatic environment*. Springer.

Garg, U. K., Kaur, M., Sud, D., & Garg, V. (2009). Removal of hexavalent chromium from aqueous solution by adsorption on treated sugarcane bagasse using response surface methodological approach. *Desalination*, 249(2), 475–479.

Gilliland, E. R., Baddour, R. F., Perkinson, G. P., & Sladek, K. J. (1974). Diffusion on surfaces. I. Effect of concentration on the diffusivity of physically adsorbed gases. *Industrial & Engineering Chemistry Fundamentals*, 13(2), 95–100.

Graham, D. (1953). The characterization of physical adsorption systems. I. The equilibrium function and standard free energy of adsorption. *The Journal of Physical Chemistry*, 57(7), 665–669.

Guan, X., Sun, Y., Qin, H., Li, J., Lo, I. M., He, D., & Dong, H. (2015). The limitations of applying zero-valent iron technology in contaminants sequestration and the corresponding countermeasures: The development in zero-valent iron technology in the last two decades (1994–2014). *Water Research*, 75, 224–248.

Hamdy, A., Mostafa, M., & Nasr, M. (2019). Regression analysis and artificial intelligence for removal of methylene blue from aqueous solutions using nanoscale zero-valent iron. *International Journal of Environmental Science and Technology*, 16(1), 357–372.

He, B., Yun, Z., Shi, J., & Jiang, G. (2013). Research progress of heavy metal pollution in China: Sources, analytical methods, status, and toxicity. *Chinese Science Bulletin*, 58(2), 134–140.

He, Y., Lin, H., Dong, Y., Li, B., Wang, L., Chu, S., . . . Liu, J. (2018). Zeolite supported Fe/Ni bimetallic nanoparticles for simultaneous removal of nitrate and phosphate: Synergistic effect and mechanism. *Chemical Engineering Journal*, 347, 669–681.

Ho, Y.-S., & McKay, G. (1998a). A comparison of chemisorption kinetic models applied to pollutant removal on various sorbents. *Process Safety and Environmental Protection*, 76(4), 332–340.

Ho, Y.-S., & McKay, G. (1998b). Kinetic models for the sorption of dye from aqueous solution by wood. *Process Safety and Environmental Protection*, 76(2), 183–191.

Ho, Y.-S., & McKay, G. (1999). Pseudo-second order model for sorption processes. *Process Biochemistry*, 34(5), 451–465.

Hu, J., Chen, G., & Lo, I. M. (2005). Removal and recovery of Cr (VI) from wastewater by maghemite nanoparticles. *Water Research*, 39(18), 4528–4536.

Jain, M., Yadav, M., Kohout, T., Lahtinen, M., Garg, V. K., & Sillanpää, M. (2018). Development of iron oxide/activated carbon nanoparticle composite for the removal of Cr (VI), Cu (II) and Cd (II) ions from aqueous solution. *Water Resources and Industry*, 20, 54–74.

Jaishankar, M., Tseten, T., Anbalagan, N., Mathew, B. B., & Beeregowda, K. N. (2014). Toxicity, mechanism and health effects of some heavy metals. *Interdisciplinary Toxicology*, 7(2), 60–72.

Karabay, S. (2008). *Waste management in leather industry.* DEÜ Fen Bilimleri Enstitüsü.

Kurniawan, A., Sisnandy, V. O. A., Trilestari, K., Sunarso, J., Indraswati, N., & Ismadji, S. (2011). Performance of durian shell waste as high capacity biosorbent for Cr (VI) removal from synthetic wastewater. *Ecological Engineering*, 37(6), 940–947.

Langat, N. K. (2018). *Isolation and molecular characterization of chromium reducing bacterial strains from selected chrome contaminated tannery waste sites in Nairobi, Kenya.* Institute for Biotechnology Research, Jomo Kenyatta University of Agriculture and Technology.

Larson-Hall, J. (2015). *A guide to doing statistics in second language research using SPSS and R.* Routledge.

Li, J., Fan, M., Li, M., & Liu, X. (2020). Cr (VI) removal from groundwater using double surfactant-modified nanoscale zero-valent iron (nZVI): Effects of materials in different status. *Science of the Total Environment*, 717, 137112.

Li, Z., Ma, Z., van der Kuijp, T. J., Yuan, Z., & Huang, L. (2014). A review of soil heavy metal pollution from mines in China: Pollution and health risk assessment. *Science of the Total Environment*, 468, 843–853.

Lin, N., & Dufresne, A. (2013). Physical and/or chemical compatibilization of extruded cellulose nanocrystal reinforced polystyrene nanocomposites. *Macromolecules*, 46(14), 5570–5583.

Low, K.-S., Lee, C.-K., & Lee, C.-Y. (2001). Quaternized wood as sorbent for hexavalent chromium. *Applied Biochemistry and Biotechnology*, 90(1), 75–87.

Lu, Y., Song, S., Wang, R., Liu, Z., Meng, J., Sweetman, A. J., . . . Luo, W. (2015). Impacts of soil and water pollution on food safety and health risks in China. *Environment International*, 77, 5–15.

Lucas, F., Trindade, B., Costa, B. F., & Le Caër, G. (2002). Mechanical alloying of Fe-Cu alloys from As-received and premilled elemental powder mixtures. *Key Engineering Materials*, 230–232, 631–634.

Luo, C., Tian, Z., Yang, B., Zhang, L., & Yan, S. (2013). Manganese dioxide/iron oxide/acid oxidized multi-walled carbon nanotube magnetic nanocomposite for enhanced hexavalent chromium removal. *Chemical Engineering Journal*, 234, 256–265.

Lv, X., Xu, J., Jiang, G., Tang, J., & Xu, X., (2012). Highly active nanoscale zero-valent iron (nZVI)–Fe3O4 nanocomposites for the removal of chromium (VI) from aqueous solutions. *Journal of Colloid and Interface Science*, 369(1), 460–469.

Mahmoud, A. S. (2017). *Study the removal of most hazardous pollutants from aqueous solutions using nanoparticles.* http://lis.cl.cu.edu.eg/search*ara

Mahmoud, A. S., Farag, R. S., & Elshfai, M. M. (2020). Reduction of organic matter from municipal wastewater at low cost using green synthesis nano iron extracted from black tea: Artificial intelligence with regression analysis. *Egyptian Journal of Petroleum*, 29(1), 9–20.

Mahmoud, A. S., Farag, R. S., Elshfai, M. M., Mohamed, L. A., & Ragheb, S. M. (2019). Nano zero-valent aluminum (nZVAl) preparation, characterization, and application for the removal of soluble organic matter with artificial intelligence, isotherm study, and kinetic analysis. *Air, Soil and Water Research*, 12, 1–13.

Mahmoud, A. S., Ismail, A., Mostafa, M. K., Mahmoud, M., Ali, W., & Shawky, A. M. (2020). Isotherm and kinetic studies for heptachlor removal from aqueous solution using Fe/Cu nanoparticles, artificial intelligence, and regression analysis. *Separation Science and Technology*, 55(4), 684–696.

Mahmoud, A. S., Mostafa, M. K., & Abdel-Gawad, S. A. (2018). Artificial intelligence for the removal of benzene, toluene, ethyl benzene and xylene (BTEX) from aqueous solutions using iron nanoparticles. *Water Supply*, 18(5), 1650–1663.

Mahmoud, A. S., Mostafa, M. K., & Nasr, M. (2019). Regression model, artificial intelligence, and cost estimation for phosphate adsorption using encapsulated nanoscale zero-valent iron. *Separation Science and Technology*, 54(1), 13–26.

Masindi, V., & Muedi, K. L. (2018). Environmental contamination by heavy metals. *Heavy Metals*, 10, 115–132.

Mekonnen, E., Yitbarek, M., & Soreta, T. R. (2015). Kinetic and thermodynamic studies of the adsorption of Cr (VI) onto some selected local adsorbents. *South African Journal of Chemistry*, 68, 45–52.

Meyers, J., & Liapis, A. (1999). Network modeling of the convective flow and diffusion of molecules adsorbing in monoliths and in porous particles packed in a chromatographic column. *Journal of Chromatography A*, 852(1), 3–23.

Mohan, D., Singh, K. P., & Singh, V. K. (2008). Wastewater treatment using low cost activated carbons derived from agricultural byproducts—A case study. *Journal of Hazardous Materials*, 152(3), 1045–1053.

Mostafa, M. K., Mahmoud, A. S., Saryel-Deen, R. A., & Peters, R. W. (2017, October 29–November 3). *Application of entrapped nano zero valent iron into cellulose acetate membranes for domestic wastewater treatment* [Paper presentation]. The Environmental Aspects, Applications and Implications of Nanomaterials and Nanotechnology 2017–Topical Conference at the 2017 AIChE Annual Meeting, Minneapolis, MN, United States.

Mostafa, M. K., & Peters, R. W. (2016). Improve effluent water quality at Abu-Rawash wastewater treatment plant with the application of coagulants. *Water and Environment Journal*, 30(1–2), 88–95.

Mutongo, F., Kuipa, O., & Kuipa, P. K. (2014). Removal of Cr (VI) from aqueous solutions using powder of potato peelings as a low cost sorbent. *Bioinorganic Chemistry and Applications*, 2014, 973153.

Mystrioti, C., Sparis, D., Papasiopi, N., Xenidis, A., Dermatas, D., & Chrysochoou, M. (2015). Assessment of polyphenol coated nano zero valent iron for hexavalent chromium removal from contaminated waters. *Bulletin of Environmental Contamination and Toxicology*, 94(3), 302–307.

Nriagu, J. O. (1988). Production and uses of chromium. *Chromium in the Natural and Human Environments*, 20, 81–104.

Omar, H. D. (2016). The analysis of copper-iron metallic mixture by means of XRD and XRF. *International Letters of Chemistry, Physics and Astronomy*, 64, 130–134.

Owalude, S. O., & Tella, A. C. (2016). Removal of hexavalent chromium from aqueous solutions by adsorption on modified groundnut hull. *Beni–Suef University Journal of Basic and Applied Sciences*, 5(4), 377–388.

Peng, H., & Guo, J. (2020). Removal of chromium from wastewater by membrane filtration, chemical precipitation, ion exchange, adsorption electrocoagulation, electrochemical reduction, electrodialysis, electrodeionization, photocatalysis and nanotechnology: A review. *Environmental Chemistry Letters*, 18, 2055–2068.

Pradhan, J., Das, S. N., & Thakur, R. S. (1999). Adsorption of hexavalent chromium from aqueous solution by using activated red mud. *Journal of Colloid and Interface Science*, 217(1), 137–141.

Saryel-Deen, R. A., Mahmoud, A. S., Mahmoud, M., Mostafa, M. K., & Peters, R. W. (2017, October 29–November 3). *Adsorption and kinetic studies of using entrapped sewage sludge ash in the removal of chemical oxygen demand from domestic wastewater, with artificial intelligence approach* [Paper presentation]. The Annual AIChE Meeting, Minneapolis, MN, United States.

Selvi, K., Pattabhi, S., & Kadirvelu, K. (2001). Removal of Cr (VI) from aqueous solution by adsorption onto activated carbon. *Bioresource Technology*, 80(1), 87–89.

Stefaniuk, M., Oleszczuk, P., & Ok, Y. S. (2016). Review on nano zerovalent iron (nZVI): From synthesis to environmental applications. *Chemical Engineering Journal*, 287, 618–632.

Water Environment Federation, American Public Health Association. (2005). *Standard methods for the examination of water and wastewater.* American Public Health Association.

Weng, C.-H., Lin, Y.-T., & Tzeng, T.-W. (2009). Removal of methylene blue from aqueous solution by adsorption onto pineapple leaf powder. *Journal of Hazardous Materials*, 170(1), 417–424.

Wuana, R. A., & Okieimen, F. E. (2011). Heavy metals in contaminated soils: A review of sources, chemistry, risks and best available strategies for remediation. *ISRN Ecology*, 2011, 402647.

Yuan, P., Fan, M., Yang, D., He, H., Liu, D., Yuan, A., . . . Chen, T. (2009). Montmorillonite-supported magnetite nanoparticles for the removal of hexavalent chromium [Cr (VI)] from aqueous solutions. *Journal of Hazardous Materials*, 166(2–3), 821–829.

Yuan, P., Liu, D., Fan, M., Yang, D., Zhu, R., Ge, F., . . . He, H. (2010). Removal of hexavalent chromium [Cr (VI)] from aqueous solutions by the diatomite-supported/unsupported magnetite nanoparticles. *Journal of Hazardous Materials*, 173(1–3), 614–621.

Zeldowitsch, J. (1934a). Adsorption site energy distribution. *Acta Physicochimica URSS*, 1, 961–973.

Zeldowitsch, J. (1934b). Mechanism of the catalytic oxidation of CO an MnO2. *Acta Physicochimica URSS*, 1, 364–449.

Zhou, S., Li, Y., Chen, J., Liu, Z., Wang, Z., & Na, P. (2014). Enhanced Cr (VI) removal from aqueous solutions using Ni/Fe bimetallic nanoparticles: Characterization, kinetics and mechanism. *RSC Advances*, 4(92), 50699–50707.

Zhou, T., Li, Y., & Lim, T.-T. (2010). Catalytic hydrodechlorination of chlorophenols by Pd/Fe nanoparticles: Comparisons with other bimetallic systems, kinetics and mechanism. *Separation and Purification Technology*, 76(2), 206–214.

Zin, M. T., Borja, J., Hinode, H., & Kurniawan, W. (2013). Synthesis of bimetallic Fe/Cu nanoparticles with different copper loading ratios. *Dimensions*, 13(19), 1031–1035.